Bull. Mater. Sci., Vol. 39, No. 1, February 2016, pp. 47–55. © Indian Academy of Sciences.

Carbon nanotubes dispersed polymer nanocomposites: mechanical, electrical, thermal properties and surface morphology

NITIN SANKAR, MAMILLA NAGARJUN REDDY and R KRISHNA PRASAD*
Department of Chemical Engineering & Materials Science, Center of Excellence in Advanced Materials & Green Technology, Amrita Vishwa Vidyapeetham University, Ettimadai, Coimbatore 641 112, India

MS received 2 July 2015; accepted 27 August 2015

Abstract. **The various properties and surface morphology of the carbon nanotubes (CNTs) dispersed polydimethyl siloxane (PDMS) matrix were studied to determine their usefulness in various applications. The tensile strength, Young's modulus and electrical breakdown strength of CNT/polymer composites were 0.35 MPa, 1.2 MPa and 8.1 kV, respectively. The thermal conductivity and dielectric constant for the material having 4.28 wt% CNT were 0.225 W m^{-1} K^{-1} and 2.329, respectively. The CNT/polymer composites are promising functional composites with improved mechanical and electrical properties. The scanning electron microscope analysis of surface morphology of PDMS/CNT composite showed that the rough surface texture on nanocomposite has large surface area with circular pores. The Fourier transform infrared spectroscopy showed the functional groups present in polymer nanocomposite.**

Keywords. **Carbon nanotubes; nanocomposite; Young's modulus; breakdown strength; dielectric constant; thermal conductivity.**

1. Introduction

The polymer composite has material characteristics useful for diverse applications such as capacitors and acoustic emission sensors. The nanoscaled fillers are dispersed in polymers to improve their conductivity [1]. The nanocomposite materials have polymer matrix reinforced by separate nanomaterial to improve their properties [2]. The polymers are filled with particles that improve their stiffness and toughness of material, enhance barrier properties, and improve their resistance to fire [3]. The polymers are mostly reinforced by fillers to increase their mechanical, optical, and electrical properties and also to introduce antibacterial properties to the material [4].

The nanosized particles are distributed in polymer to occupy large number of sites in the polymer matrix to improve their strength and other properties. The reinforcement with nanoparticle improves the properties such as modulus, heat resistance, electrical conductivity, and structural strength but reduces gas permeability and flammability [5,6]. The reinforcement with nanocomposite improves the UV shielding and UV resistance of transparent polymers [7]. The particle agglomerations of nanoparticles are avoided by incorporating them in polymer matrix [8]. The polymer nanocomposite has wide applications in the field of microwave absorbing, data storage, sensors, and biomedical applications [9].

The polydimethylsiloxane (PDMS) and multi-walled carbon nanotube (MWCNT) nanocomposite have elastomeric nanocomposite feature in photosimulated mechanical response [10] and applied in fields such as electronic packaging material and angular acceleration accelerometers [11]. The PDMS is a silicon-based organic polymer composed of a repeating $[SiO(CH_3)_2]$ unit and is in rubber state at room temperature as its glass transition temperature is less than −120°C. It possesses hydrophobic, non-conductive, and biocompatible properties useful in various applications such as casting moulds and micro-fluidic devices and also useful in medical devices owing to properties such as oxygen permeability, optical transparency, and self-healing property [12]. Young's modulus of PDMS can be reduced by reducing the relative amount of curing agent to base material while mixing the polymer [13]. The PDMS exists as clear, colourless, viscous, and transparent liquid [14] and is a hyperelastic polymer that undergoes big distortions without deteriorations [15,16].

The carbon nanotubes (CNTs) consist of graphene sheets rolled to form a tube which exist as multi-walled, double-walled, and single-walled CNTs depending on layers of graphene sheets [17,18]. The electrical current carrying capacity of CNT is thousand times larger than a copper wire. CNT has high strength, toughness, large surface area, and hollow geometry [19,20]. CNTs are reinforcement materials adding multifunctionality to a composite system as they have excellent mechanical, electrical, and optical properties along with their ability to adhere to chemical species or functional groups [21–24]. The incorporation of CNT into polymer improves their tensile strength, toughness, glass transition temperature, thermal conductivity, electrical conductivity, and optical properties [25–27]. The PDMS/CNT nanocomposites

*Author for correspondence (rkprasad_cbe@rediffmail.com)

are prepared by different techniques such as emulsion polymerization, electrospinning, melt blending, bulk polymerization, *in-situ* polymerization, intercalation of polymer from solution, dispersion destabilization and exfoliation [28]. The effect of surfactant and MWCNTs in a silicone matrix were studied by several researchers [29]. In this study dispersion of CNT on PDMS is achieved by solution mixing with chloroform as solvent.

2. Materials and methods

The PDMS procured from Dow Corning as Sylgard 184 elastomer kit consisting of elastomer and curing agent and the MWCNT procured from Nanoshel has diameter of 20–39 nm, length of 15–30 μm, and relative purity of >95%. The MWCNT is mixed with 200 ml of chloroform in ultrasonicator for an hour and PDMS with 40 ml of chloroform in a magnetic stirrer for 15 min and both these mixtures were mixed in ultrasonicator for 1–2 h. The ultrasonicated mixture was kept in oven at 62°C for 4 h to evaporate the solvent. The base polymer to curing agent ratio added was 10 : 1 and the mixture was transferred to a tray to obtain correct shape, length, thickness, and kept in oven at 150°C to cure the nanocomposite.

The tensile strength and Young's modulus were determined by conducting tensile test using universal testing machine. The tensile strength was recorded directly and Young's modulus was calculated from the stress–strain curve obtained from the test. The breakdown strength was determined by conducting breakdown test using a transformer oil test set.

Table 1. The experimental range of factors studied in preparation of PDMS–CNT nanocomposite.

Factors	Minimum value	Maximum value
Amount of MWCNT (g/50 ml solvent) X_1	0.2	0.3
g of PDMS/ml of solvent X_2	0.5	0.7
Time of sonication (h) X_3	1	2

The experimental range of factors studied are amount of MWCNT (X_1), amount of PDMS (X_2) and time of sonication (X_3) as given in table 1. The factorial design model used to determine various responses like tensile strength (Y_1), Young's modulus (Y_2) and breakdown strength (Y_3) is expressed as follows:

$$Y = \beta_0 + \beta_1 X_1 + \beta_2 X_2 + \beta_3 X_3 + \beta_{11} {X_1}^2 + \beta_{22} {X_2}^2 + \beta_{33} {X_3}^2 + \beta_{12} X_1 X_2 + \beta_{13} X_1 X_3 + \beta_{23} X_2 X_3,$$

where Y is the predicted response; β_0 the model constant; β_1, β_2 and β_3 the linear coefficients; β_{11}, β_{22} and β_{33} the quadratic or square coefficients; β_{12}, β_{13} and β_{23} the cross product or interaction coefficients. X_1, X_2 and X_3 are various parameters studied. The Fourier transform infrared spectroscopy (FT-IR) was recorded using Thermo Nicolet is 10 FT-IR spectrometer using KBr pellets in the range of 500–4000 cm^{-1}. The scanning electron microscope (SEM) analysis was carried out using SEM VEGA3 TESCAN instrument operated at acceleration voltage of 5 and 30 kV to analyse the surface morphology of PDMS–MWCNT nanocomposite.

The thermal conductivity was determined by conducting experiment in Hot Disk PPS-2500S instrument. The storage and loss modulus were recorded using DMA6100 HITACHI instrument. The thermal stability was analysed by using TGA-6200 HITACHI instrument and the dielectric constant was determined by dielectric constant meter at 1 MHz at 30°C. The electrical conductivity was measured by electric conductometer instrument. The X-ray diffraction (XRD) was recorded using Pan analytica at 40 kV and 30 mA.

3. Results and discussions

3.1 *Process model and contour regions of tensile strength in polymeric nanocomposite*

The tensile strength, Young's modulus, and breakdown strength of PDMS/CNT composite for eight sets of nanocomposites prepared are given in table 2. The regression correlation

Table 2. Tensile strength, Young's modulus and breakdown strength for design of experiments studied in preparation of PDMS–CNT nanocomposite.

Amount of MWCNT (g/50 ml solvent)	g of PDMS/ 10 ml of solvent	Time of sonication (h)	Tensile strength (MPa)	Young's modulus (MPa)	Breakdown strength (kV)
0.2	7	2	0.0214	0.38	7.4
0.2	7	1	0.1214	0.78	7
0.2	5	1	0.1929	0.58	7.2
0.3	7	2	0.0929	0.49	7.6
0.3	5	1	0.3571	1.038	7
0.3	7	1	0.2643	1.26	7.5
0.2	5	2	0.1214	0.34	8.5
0.3	5	2	0.1429	0.342	7.5

for tensile strength irrespective of significances is expressed as follows:

$$\begin{aligned}\text{Tensile strength: } Y_1 = &-0.7049 + 5.384X_1 \\ &+ 0.071X_2 + 0.6416X_3 \\ &- 0.463X_1X_2 - 3.2X_1X_3 \\ &- 0.085X_2X_3 + 0.3565X_1X_2X_3.\end{aligned}$$

The maximum amount of tensile stress which a material can withstand before failure is known as its tensile strength. The tensile strength of a material provides the extent to which a material can be stretched. The contour plot of tensile strength as a function of change in amount of MWCNT and dispersion time is shown in figure 1 which provides maximum tensile strength of 0.3 MPa in nanocomposite with 0.26–0.30 g MWCNT dispersion in PDMS for an hour of ultrasonication. The contour plot shown in figure 2 represents the operating regions of amount of MWCNT dispersed in PDMS having tensile strength of 0.3 MPa for 0.3 g MWCNT dispersed in 5–6 g PDMS. The interactions of various factors on tensile strength are shown in figure 3 which provides that the tensile stress improved with the addition of MWCNT and reduced with the increase in amount of PDMS and dispersion time.

3.2 *Contour analysis and interactions of Young's modulus in PDMS/MWCNT nanocomposite*

The regression correlation for Young's modulus based on uncoded units irrespective of significances is expressed as follows:

$$\begin{aligned}\text{Young's modulus: } Y_2 = &-2.228 + 10.74X_1 \\ &+ 0.244X_2 + 1.502X_3 \\ &- 0.32X_1X_2 - 6.71X_1X_3 \\ &- 0.166X_2X_3 + 0.43X_1X_2X_3.\end{aligned}$$

Young's modulus of material measures the material's elasticity. Figure 4 shows the operating regions of amount of MWCNT mixed with PDMS provides Young's modulus of 1.2 MPa for dispersion of MWCNT (0.28–0.3 g) in PDMS (6.5–7 g). The contour plot shown in figure 5 represents the amount of MWCNT and dispersion time provides Young's modulus of 0.9 MPa for 0.27–0.3 g MWCNT dispersion in PDMS for an hour. Young's modulus of PDMS/CNT nanocomposites was improved with the increase in amount of MWCNT as observed from figure 6 which provides the interactions of various factors on Young's modulus.

3.2a *Dynamic mechanical analysis*: The dynamic mechanical properties of PDMS/CNT nanocomposite samples four and five are shown in figures 7 and 8, respectively. The dynamic mechanical properties of PDMS/CNT nanocomposite are determined by dynamic storage and loss moduli. Storage modulus (E') is the stress in phase in a sinusoidal deformation divided by strain. The loss modulus (E'') is defined as the stress 90° out of phase with the strain divided by the strain. It is a measure of energy lost as heat per cycle of sinusoidal deformation when different systems are compared at the same strain amplitude

$$E^* = E' + \mathrm{i}E''.$$

3.3 *Contour regions and interactions of breakdown strength of polymeric nanocomposite*

The regression correlation for breakdown strength based on uncoded units irrespective of significances is expressed as follows:

$$\begin{aligned}\text{Breakdown strength: } Y_3 = &\ 3.95 + X_1 + 0.15X_2 \\ &+ 7.656X_3 + X_1X_2 \\ &- 20.5X_1X_3 - 0.95X_2X_3 \\ &+ 2.5X_1X_2X_3.\end{aligned}$$

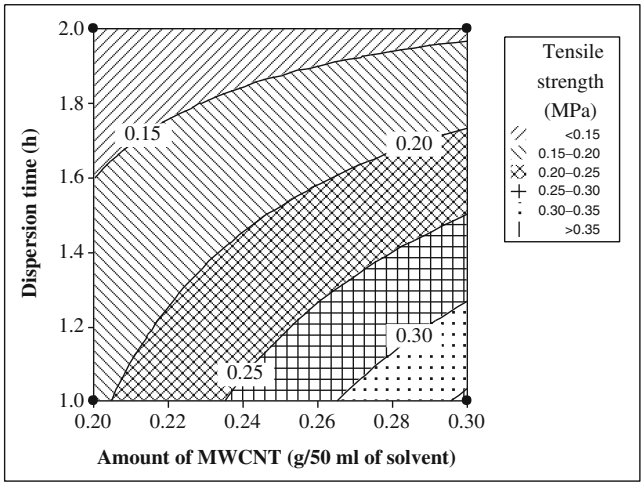

Figure 1. Contour plot of tensile strength *vs.* dispersion time and amount of MWCNT.

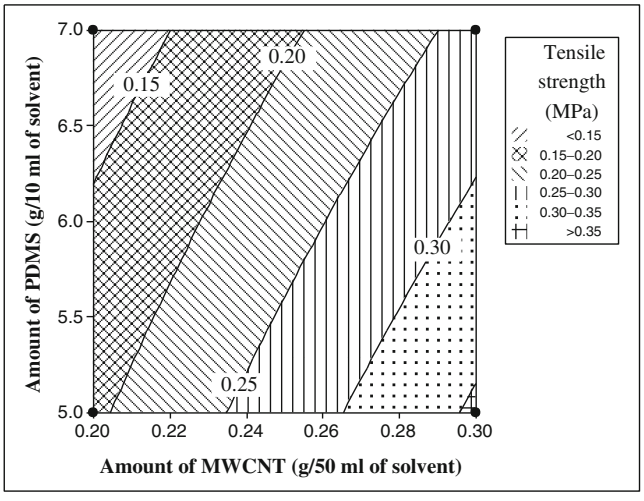

Figure 2. Contour plot of tensile strength *vs.* amount of PDMS and amount of MWCNT.

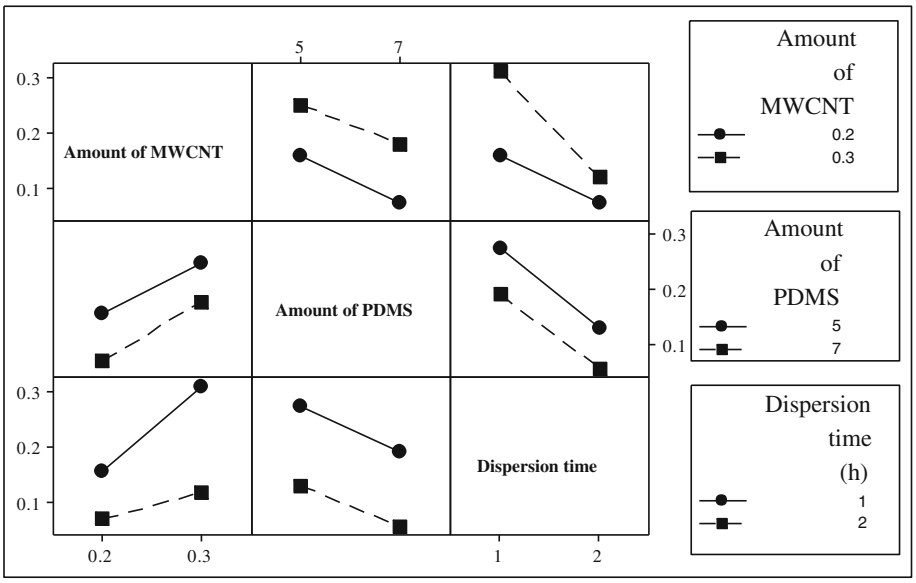

Figure 3. Interaction plot for tensile strength.

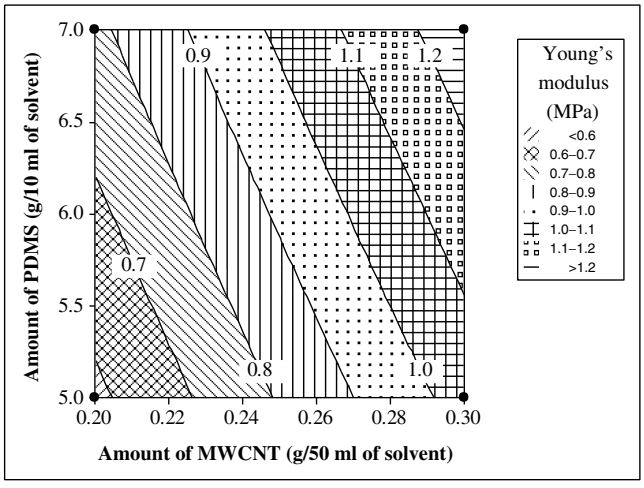

Figure 4. Contour plot of Young's modulus *vs.* amount of PDMS and amount of MWCNT.

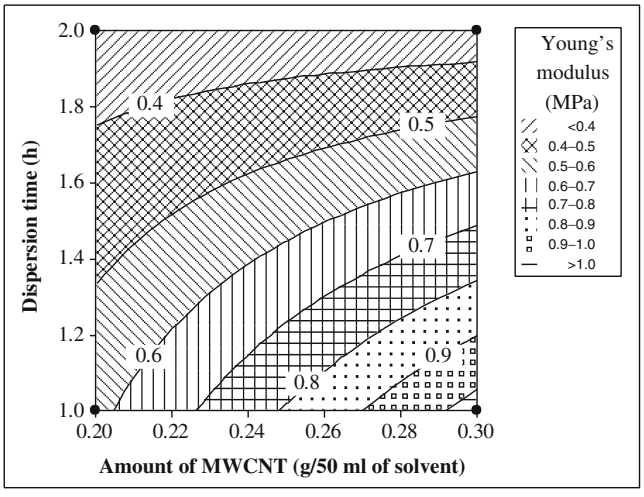

Figure 5. Contour plot of Young's modulus *vs.* dispersion time and amount of MWCNT.

The breakdown strength is the maximum electric field a material can withstand without breaking down. The contour region shown in figure 9 indicates maximum breakdown strength of 8.1 kV for dispersion of 0.28–0.3 g MWCNT in 6.5–7 g PDMS matrix. The contour region of amount of MWCNT and dispersion time is shown in figure 10 provides maximum breakdown voltage of 8.1 kV for 2 h ultrasonication of nanocomposite. It is observed from interaction matrix that breakdown strength shown in figure 11 has positive effect with the increase in amount of MWCNT and dispersion time.

3.4 *FT-IR of PDMS/CNT nanocomposite*

The FT-IR spectral analysis of PDMS/CNT nanocomposite for fifth set of design of experiments is shown in figure 12. The major peaks of synthesized nanocomposite belonged to C–H and O–H (2961 cm^{-1}), C=C and CH_3 bending vibration (1412 cm^{-1}), Si–CH_2–Si and C–O stretching (1011 cm^{-1}), Si–CH_2–CH=CH_2 (910 cm^{-1}), C–C (842 cm^{-1}), CH and OH bending vibrations (687 cm^{-1}). The Si–CH_3 group is recognized by a sharp band at 1260 cm^{-1} and another strong band in the 865–750 cm^{-1} range. This indicates the presence of polysiloxane group present in polydimethylsiloxane. The peak at 2961 cm^{-1} is due to –CH_2 and –CH_3 stretching and the peak at 1011 cm^{-1} is attributed to Si–O plane stretching.

3.5 *Estimation of properties of polymeric nanocomposites*

3.5a *Thermal stability*: The thermogravimetric analysis (TGA) for fourth and fifth set of PDMS/CNT nanocomposite

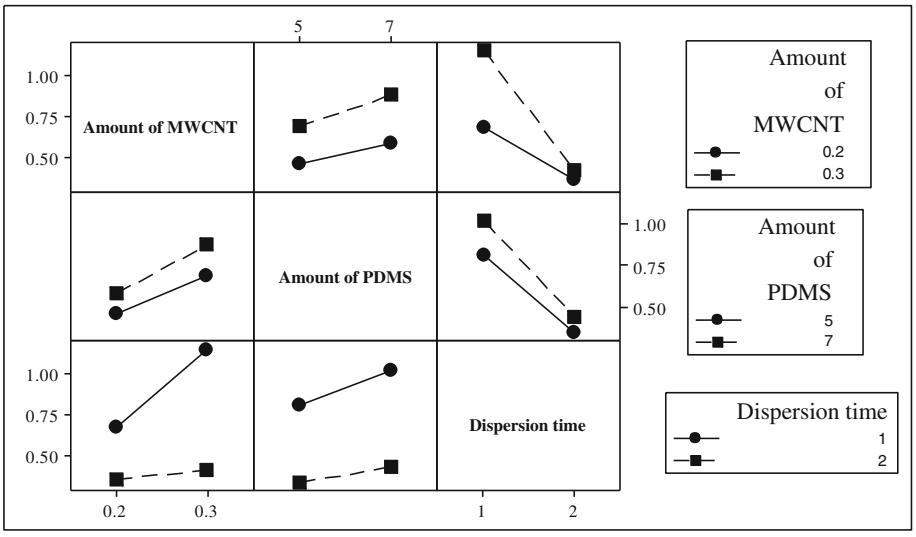

Figure 6. Interaction plot for Young's modulus.

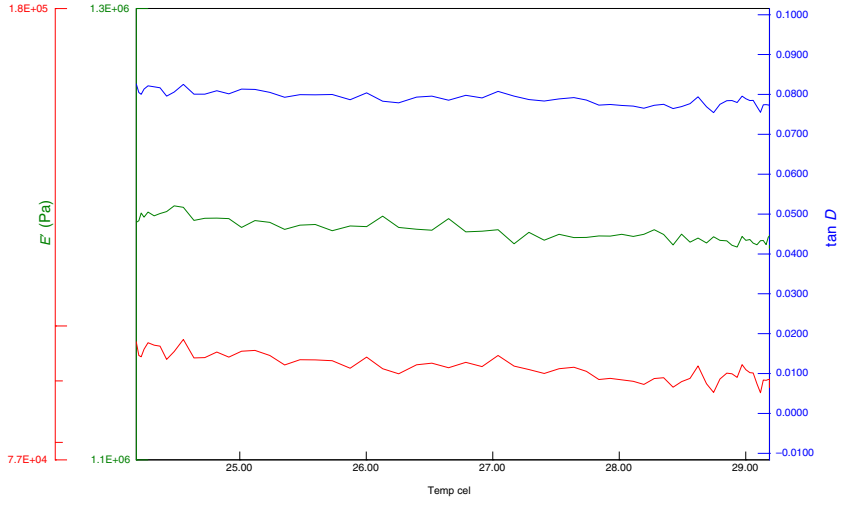

Figure 7. Dynamic mechanical properties for 0.3 g MWCNT dispersion (Sample 4).

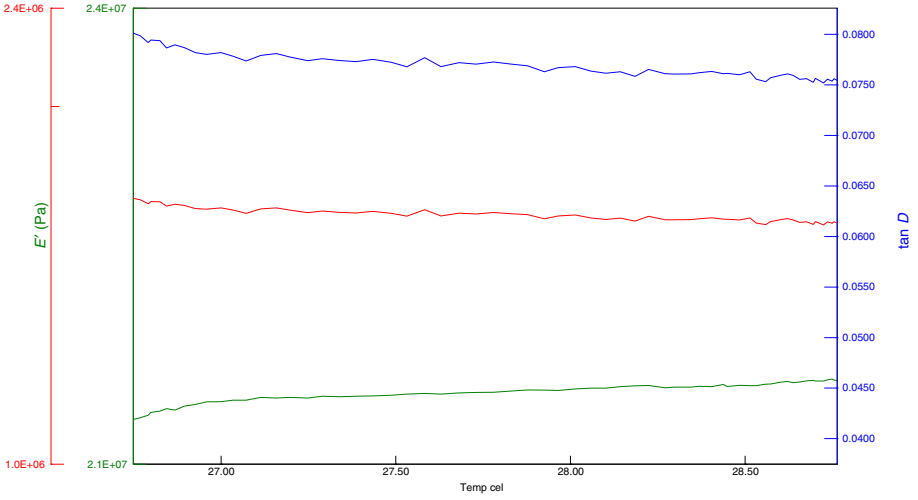

Figure 8. Dynamic mechanical properties for 0.3 g MWCNT dispersion (Sample 5).

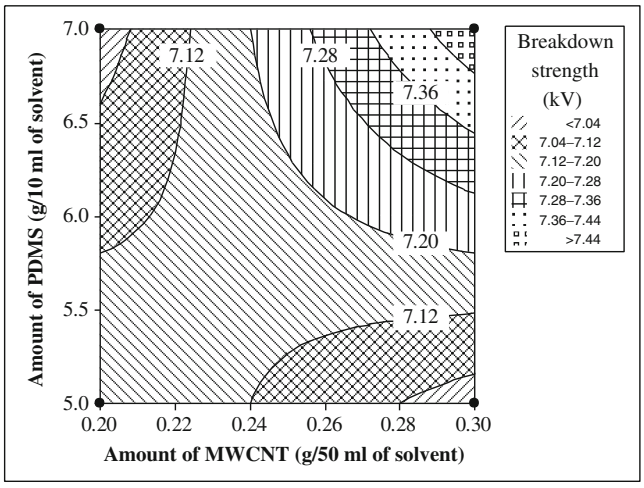

Figure 9. Contour plot of breakdown strength *vs.* amount of PDMS and amount of MWCNT.

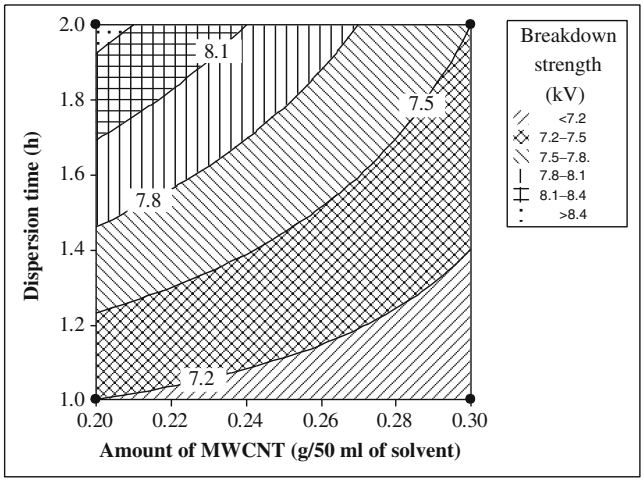

Figure 10. Contour plot of breakdown strength *vs.* dispersion time and amount of MWCNT.

was performed. The thermal stability of a material is described as resistance to decomposition at high temperatures. The specimen with 4.28 wt% MWCNT has thermal stability of 273°C and the specimen with 6 wt% MWCNT has thermal stability of 322°C. The thermal stability of PDMS/CNT nanocomposites improves with the increase in MWCNT. The presence of CNT within the PDMS matrix increases the thermal stability and electrical conductivity. The improvements in thermal stability are concurrent with the relative loading of CNT within PDMS matrix. Nanotubes have structural perfection, high electrical conductivity and chemical stability.

3.5b *Thermal conductivity*: The thermal conductivity of a material is described as the property to conduct heat. The thermal conductivity for fourth set of PDMS/CNT nanocomposite with 4.28% MWCNT is 0.225 W m^{-1} K^{-1}.

3.5c *Electrical conductivity*: The electrical conductivity analysis for PDMS/CNT nanocomposite of fourth and fifth set is recorded. The electrical conductivity of a material is described as the degree to which a specified material can conduct electricity. The electrical conductivity of the specimen with 4.28 wt% MWCNT is 2.24 $\times$ 10^{13} Ω m and for the specimen with 6 wt% MWCNT is 4.65 $\times$ 10^{13} Ω m. The electrical conductivity of PDMS/CNT improves with the increase in MWCNT.

3.5d *Dielectric constant*: The dielectric constant for PDMS/CNT nanocomposite of fourth and fifth set was measured. The dielectric constant of a material is a quantity measuring the ability to store electrical energy in an electrical field. The dielectric constant of specimen with 4.28 wt% MWCNT is 2.329 and for specimen with 6 wt% MWCNT is 11.753. The dielectric constant improves with the increase in MWCNT.

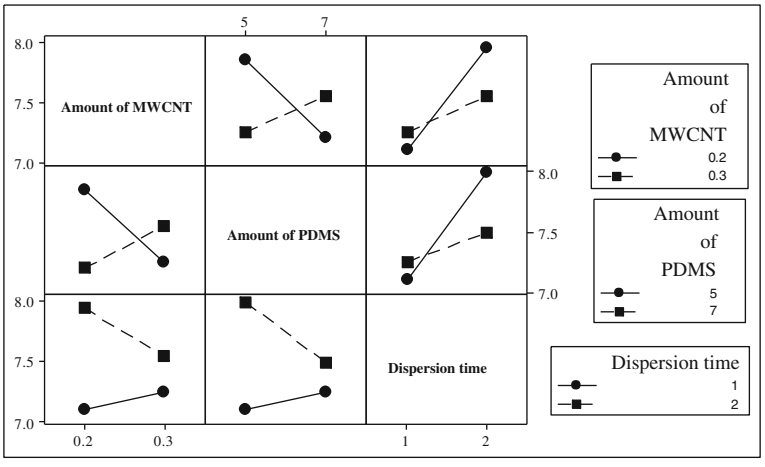

Figure 11. Interaction plot for breakdown strength.

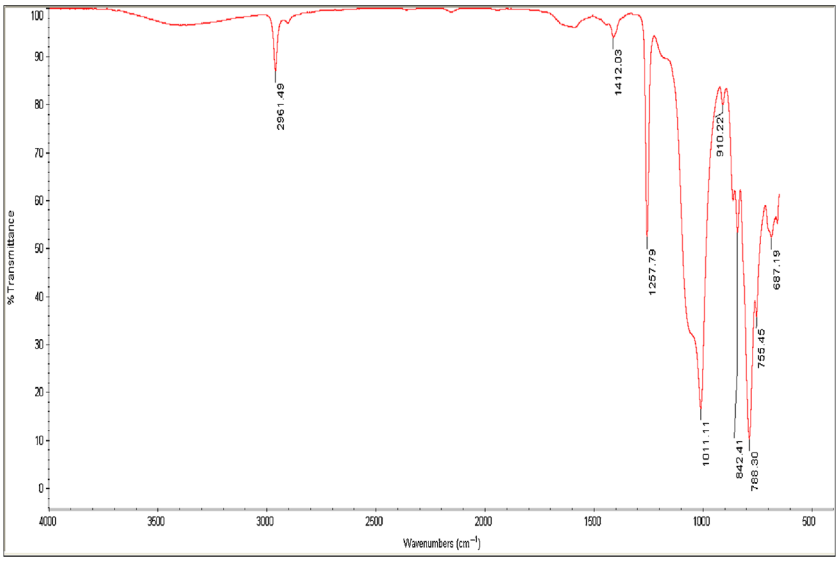

Figure 12. FT-IR spectral analysis of PDMS–CNT nanocomposite (Set 5: Amount of MWCNT = 0.3 g/50 ml solvent, amount of PDMS = 5 g of PDMS/10 ml of solvent, and time of sonication = 1 h).

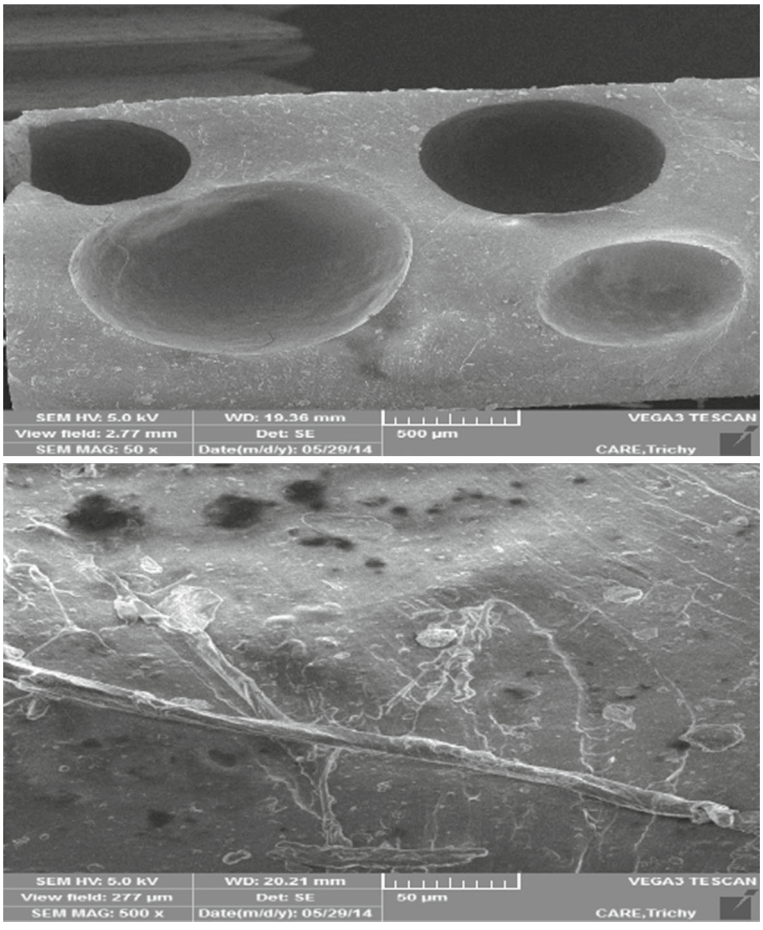

Figure 13. SEM images of PDMS–MWCNT nanocomposite (scale bar: 500 µm, 50 µm). (Set 5: Amount of MWCNT = 0.3 g/50 ml solvent, amount of PDMS = 5 g of PDMS/10 ml of solvent, and time of sonication = 1 h).

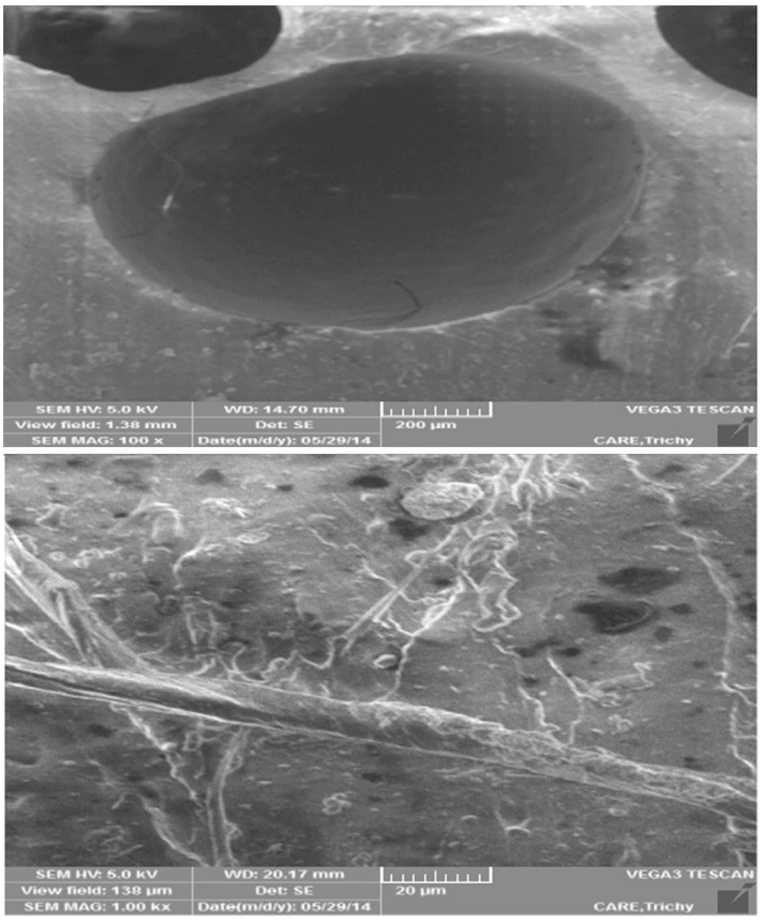

Figure 14. SEM images of PDMS–MWCNT nanocomposite (scale bar: 200 µm, 20 µm). (Set 5: Amount of MWCNT = 0.3 g/50 ml solvent, amount of PDMS = 5 g of PDMS/10 ml of solvent, and time of sonication = 1 h).

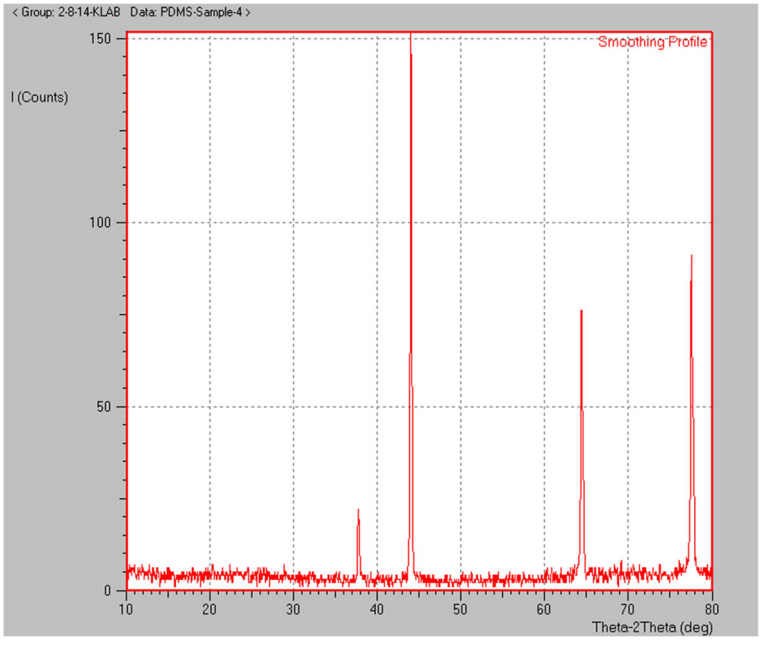

Figure 15. XRD spectra pattern of PDMS/CNT nanocomposite.

3.6 *SEM studies of PDMS/CNT nanocomposite*

The SEM images of fifth set of PDMS/CNT nanocomposite at different resolution scale bar are shown in figures 13 and 14. The SEM imaging is useful to study the surface morphology and understand surface texture. The imaging was carried out at various degrees of magnification for better analysis. The surface porosity is visible in SEM images and is as shown in figure 13 for scale bar 50 μm. The 20 μm SEM magnification shows tubular structure with crossing over as shown in figure 14. The SEM imaging at scale bar 200 and 500 μm provides detailed pore structure and size and the pores are circular in shape as seen in the images. The good bonding strength between PDMS and CNT improved Young's modulus of PDMS. The rough surface texture on nanocomposite is observed from the SEM images that have large surface area and nano sized textures useful in selective adsorption applications. XRD has been employed to help qualify the degree of shape and orientation preference. The XRD patterns of PDMS/CNT nanocomposite are presented in figure 15. XRD is used to measure in polymer nanocomposites the efficiency of intercalation in the lamellar galleries. The peaks are broadened due to microstrain or grain size broadening.

4. Conclusions

The reinforcing of PDMS polymer with MWCNT provides significant improvement in its mechanical and electrical properties. The dispersion of 0.3 g MWCNT in polymer composite resulted in tensile stress and Young's modulus of 0.35 and 1.2 MPa, respectively. The breakdown strength of PDMS/CNT composite improved with the increase in amount of MWCNT and dispersion time. The Si-CH_3 group is recognized by a sharp band at 1260 cm^{-1} in the polymer nanocomposite. The rough surface texture on nanocomposite was observed from the SEM images having large surface area and nanosized textures.

References

[1] Liu C-X and Choi J W 2012 *Nanomaterials* **2** 329

[2] Hu H, Onyebueke L and Abatan A 2010 *J. Miner. Mater. Charact. Eng.* **9** 275

[3] Alexandre M and Dubois P 2000 *Mater. Sci. Eng. R* **28** 1

[4] Ahmed D S, Haider A J and Mohammed M R 2013 *Energy Procedia* **36** 1111

[5] Huang Y Y and Terentjev E M 2012 *Polymers* **4** 275

[6] Giannelis E P 1998 *Appl. Organomet. Chem.* **12** 675

[7] Li Y-Q, Fu S-Y, Yang Y and Mai Y-W 2008 *Chem. Mater.* **20** 2637

[8] Leite E R, Carreno N L V, Longo E and Pontes F M 2002 *Chem. Mater.* **14** 3722

[9] Agarwal T, Gupta K, Zaidi M G H and Alam S 2012 *Nanosci. Nanotechnol.* **2** 5

[10] Kim T and Kim H 2010 *Korea Aust. Rheol. J.* **22** 205

[11] Nayak S, Chaki T K and Khastgir D 2013 *Adv. Mater. Res.* **622** 897

[12] King M G, Bargawanath A J, Rosamond M C, Wood D and Gallant A J 2009 *Procedia Chem.* **1** 568

[13] Talaei S, Frey O, Van Der Waal P D, De Rooij N F and Koudelka M 2009 *Procedia Chem.* **1** 381

[14] Bourbaba H, Achaiba C B and Mohammed B 2013 *Energy Procedia* **36** 231

[15] Lotters J C, Olthuis W, Veltink P H and Bergveld P 1997 *J. Micromech. Microeng.* **7** 145

[16] Punbusayakul N 2012 *Procedia Eng.* **32** 683

[17] Huang J and Rodrigue D 2014 *Mater. Des.* **55** 653

[18] Meng N and Zhou N-L 2014 *Carbohydr. Polym.* **105** 70

[19] Fang J, Shan X-Q and Huang R-X 2013 *Geoderma* **207** 1

[20] Zhao D, Zhang W, Chen C and Wang X 2013 *Procedia Environ. Sci.* **18** 890

[21] Khatiwada S, Armada C A and Barrera E V 2013 *Procedia Eng.* **58** 4

[22] Das R, Ali M E, Abd Hamid S B, Ramakrishna S and Cowdhary Z Z 2014 *Desalination* **336** 97

[23] Nguyen Q T and Baird D G 2006 *Adv. Polym. Technol.* **25** 270

[24] Li C and Shi G 2014 *J. Photochem. Photobiol.* **19** 20

[25] Huang Y Y and Terentjev E M 2012 *Polymers* **4** 275

[26] Sahoo N G, Rana S, Cho J W, Li L and Chan S H 2010 *Prog. Polym. Sci.* **35** 837

[27] Erdem Yalcinkaya S, Yildiz N, Sacak M and Calimli A 2010 *Turk. J. Chem.* **34** 581

[28] Morales-Games L, Jones I, Franco L and Puiggali J 2011 *Express Polym. Lett.* **8** 717

[29] Vilčáková J, Moučka R, Svoboda P, Ilčíková M, Kazantseva N, Hřibová M, Mičušík M and Omastová M 2012 *Molecules* **17** 13157